Development and Control of a Holonomic Mobile Robot for Mobile Manipulation Tasks

Robert Holmberg and Oussama Khatib

The International Journal of Robotics Research 2000 19: 1066
DOI: 10.1177/02783640022067977

Robert Holmberg*
Oussama Khatib

The Robotics Laboratory
Computer Science Department
Stanford University, Stanford, California, USA

Development and Control of a Holonomic Mobile Robot for Mobile Manipulation Tasks

Abstract

Mobile manipulator systems hold promise in many industrial and service applications including assembly, inspection, and work in hazardous environments. The integration of a manipulator and a mobile robot base places special demands on the vehicle's drive system. For smooth, accurate motion and coordination with an onboard manipulator, a holonomic vibration-free wheel system that can be dynamically controlled is needed. In this paper, we present the design and development of a powered caster vehicle (PCV), which is shown to possess the desired mechanical properties. To dynamically control the PCV, a new approach for modeling and controlling the dynamics of this parallel redundant system is proposed. The experimental results presented in the paper illustrate the performance of this platform and demonstrate the significance of dynamic control and its effectiveness in mobile manipulation tasks.

KEY WORDS—mobile robot, powered caster, holonomic, mobile manipulation, augmented object

1. Introduction

Our work in mobile manipulation (Khatib et al. 1996; Khatib, Yokoi, et al. 1999) started with the development of the Stanford Robotics Platforms. In collaboration with Oak Ridge National Laboratories and Nomadic Technologies, we designed and built (Khatib, Yokoi, et al. 1999) two holonomic mobile manipulator platforms. Each platform was equipped with a PUMA 560 arm and a base that consists of three "lateral" orthogonal universal-wheel assemblies (Pin and Killough 1994), allowing the base to translate and rotate holonomically in relatively flat officelike environments. The Stanford Robotics Platforms provided a unique test bed for the development, implementation, and demonstration of various mobile manipulation control strategies, collision avoidance, and cooperative manipulation (Khatib, Brock, et al. 1999). The experiments conducted with these platforms have also illustrated the limitations of the holonomic base and highlighted the need to advance its capabilities. The work presented in this paper is part of the commercial efforts of Nomadic Technologies in mobile robots and our continuing research in mobile manipulation.

A holonomic system is one in which the number of degrees of freedom is equal to the number of coordinates needed to specify the configuration of the system. In the field of mobile robots, the term *holonomic mobile robot* is applied to the abstraction called the robot, or base, without regard to the rigid bodies that make up the actual mechanism. Thus, any mobile robot with three degrees of freedom of motion in the plane has become known as a holonomic mobile robot.

Many different mechanisms have been created to achieve holonomic motion. These include various arrangements of universal or omni wheels (La 1979; Carlisle 1983), double universal wheels (Bradbury 1977), Swedish or Mecanum wheels (Ilon 1971), chains of spherical (West and Asada 1992) or cylindrical wheels (Hirose and Amano 1993), orthogonal wheels (Killough and Pin 1992), and ball wheels (West and Asada 1994).

All of these mechanisms, except for some types with ball wheels, have discontinuous wheel contact points that are a great source of vibration; primarily because of the changing support provided, and often additionally because of the discontinuous changes in wheel velocity needed to maintain smooth base motion.

These mechanisms tend to have poor ground clearance due to the use of small peripheral rollers, and/or the arrangement of the mechanism leaves some of the support structure very close to the ground. The design and actuation of these mechanisms has been driven by kinematic concerns for minimum actuation and minimal sensing to make the implementations

*and Nomadic Technologies Inc., Mountain View, CA

The International Journal of Robotics Research
Vol. 19, No. 11, November 2000, pp. 1066-1074,

of odometry and control mathematically exact. Yet, many of these designs have multiple rollers with the contact points of the wheel on the ground moving from one row to the other. These contact points are often assumed to remain stationary in the middle of each wheel. This emphasis on minimal design has led to many three-wheeled designs that are more likely to tip over, or at least lift a wheel, as performance and payload is increased. Also, the minimal use of actuators often led to complex mechanical transmissions to distribute the power to the driving elements. The designs discussed are mechanically complex; often with many moving parts, some active, some passive.

Just as a kinematic approach was used in the design of these holonomic mechanisms, the control of these mechanisms was looked at from a purely kinematic perspective. Many of the designs incorporate passive rollers without sensing of their motions, so that the dynamics of these elements cannot be accounted for. Without dynamic control, it is difficult to perform coordinated motion of a mobile base and dynamically controlled manipulator.

We present here a different type of holonomic vehicle mechanism, which we will refer to as a *powered caster vehicle* or PCV. It was conceptually described by Muir and Neuman as early as 1986 as an "omnidirectional wheeled mobile robot" having "non-redundant conventional wheels" (Muir and Neuman 1986). (A "powered office chair" may be a simpler conceptual description.) They dismissed pursuing the idea since it had the potential for actuator conflict. Others have also chosen to not implement such a design because of the difficulty of the control (West and Asada 1994). More recently, a velocity controlled powered caster prototype robot was demonstrated (Wada and Mori 1996).

A dynamically controlled, holonomic mobile robot is particularly desirable in a mobile manipulation system for many reasons. A holonomic robot makes for easier gross motion planning and navigation. It allows for full use of the null space motions of the system to improve the workspace and overall dynamic endpoint properties. A dynamically controlled mobile robot is especially important when used as the base "joints" of a mobile manipulation system so that the dynamic forces developed by the manipulator can be decoupled with *forces* generated in the base joints.

We will present the design fundamentals of a working PCV mechanism, the Nomadic Technologies XR4000, shown in Figure 1. We will also present the new framework for efficient dynamic control of a PCV. The experimental results presented in the paper will show the benefit of this control framework and its impact on the integration of the PCV in a full mobile manipulation system.

2. Design

The PCV concept provides an effective approach for the development of holonomic mobility for a number of reasons.

Fig. 1. Nomadic XR4000 and PUMA 560.

The contact points between the wheels and the ground move in a continuous manner and thus do not induce vibrations from shifting support points or discontinuous wheel velocities. The location of each contact point is well-known so that control is more exact. Each wheel mechanism contains a single non-holonomic wheel, which is large enough for good ground clearance. One final point that has not been adequately addressed is that the PCV is the only holonomic mechanism that can be designed to effectively use currently available pneumatic tires—and consequently benefit from the suspension, traction, and wear properties of this well-developed technology. Because there are no passive and, more important, no unmeasured bodies in a powered caster design, the dynamics of the system can be accurately modeled.

A PCV is composed of $n \geq 2$ powered caster modules as illustrated in Figure 2. The modules could vary in size and power from module to module, but without loss of generality, we will assume that all the modules are identical. The PCV design is defined by the strictly positive geometric parameters: wheel radius (r), caster offset (b), and wheel module placement (h, β) (see Figs. 3 and 4). Along with the mass and inertia of each component in the design, parameters that affect the system dynamics include the gear ratios and motor sizes. Values for the geometric parameters must be selected so that the area swept out by each wheel does not intersect any other. The wheels should have a large enough radius to surmount anticipated obstacles. The dynamic trade-offs involve the geometry as well as the motors and gearing. Careful selection must be made to result in a mechanism that has good

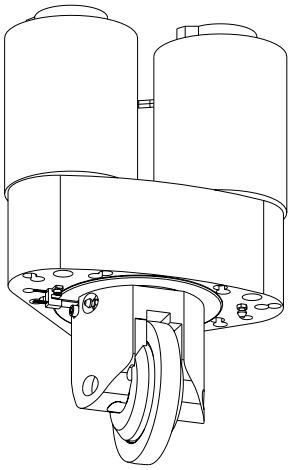

Fig. 2. Powered caster module.

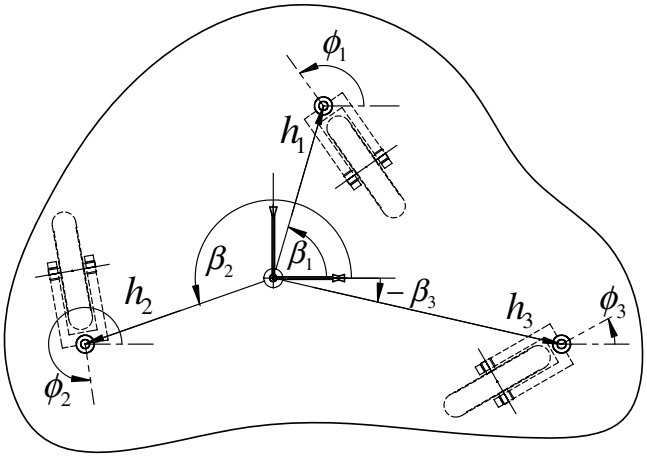

Fig. 3. Powered caster vehicle geometry.

acceleration while maintaining the ability to reach the desired top speed. At the same time, by choosing components so that motor and gearbox speeds are kept low, mechanical noise due to high component speeds can be minimized.

The PCV mechanism shown in Figure 1, a Nomadic Technologies XR4000 mobile robot, was designed to be a high-performance holonomic vehicle for mobile robotics and mobile manipulation. It has four 11 cm diameter wheels with 2 cm caster offset. It can accelerate at 2 m/s^2 on most surfaces and has a top speed of 1.25 m/s. The controller of the XR4000 used herein was modified at Stanford University by replacing the standard PWM motor amplifiers with current controlled motor amplifiers.

3. Dynamic Modeling

Typically, the dynamic equations of motion for a parallel system with nonholonomic constraints such as a PCV are formed

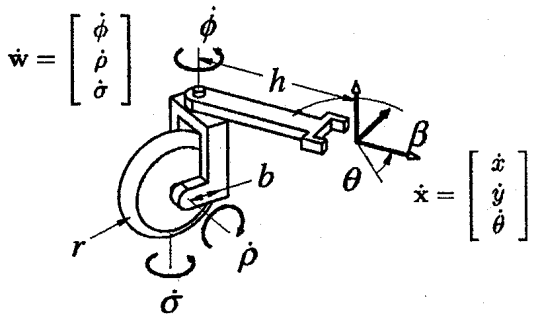

Fig. 4. Powered caster "manipulator."

in one of two ways: the unconstrained dynamics of the whole system can be derived and the constraints are applied to reduce the number of degrees of freedom (Campion, Bastin, and d'Andréa-Novel 1993), or the system is cut up into pieces, the dynamics of these subsystems are found, and the loop closure equations are used to eliminate the extra degrees of freedom. For our four-wheeled XR4000 robot, using the first method, we will obtain 11 equations for the unconstrained system and 8 constraint equations for a total of 19 equations. The second method will yield 12 equations for the unconstrained subsystems and 9 constraint equations for a total of 21 equations. These systems of equations must then be reduced to 3 equations. Ideally, both these methods would yield the same minimal set of dynamic equations but in practice it is difficult to reduce the proliferation of terms that are introduced in a large number of equations.

The PCV is treated as a collection of open-chain manipulators that will be combined to form the overall mechanism model. This is accomplished with the same concept used for multiple arms in cooperative manipulation. The open-chain mechanism is modeled, as shown in Figure 4, with steer, $\dot{\phi}$, roll, $\dot{\sigma}$, and twist at the wheel contact, $\dot{\rho}$, degrees of freedom. The dynamic equations of motion for this 3-DoF serial manipulator can be found easily and written as (Craig 1989)

$$A(\mathbf{w})\ \ddot{\mathbf{w}} + \mathbf{b}(\mathbf{w}, \dot{\mathbf{w}}) = \boldsymbol{\gamma}, \tag{1}$$

where $\mathbf{w}$ and its derivatives are the *wheel module coordinate* positions, velocities, and accelerations, A is the symmetric mass matrix, $\mathbf{b}$ is the vector of centripetal and Coriolis coupling terms, and $\boldsymbol{\gamma}$ is the joint torque vector of steer, roll, and twist torques. We assume that the PCV is on level ground and has dropped the effects of gravity.

Because of the parallel nature of the final mechanism, we choose to write the relationship between wheel module speeds and local Cartesian speeds, $\dot{\mathbf{x}}$, as

$$\dot{\mathbf{w}} = \mathbf{J}^{-1}\dot{\mathbf{x}} \tag{2}$$

$$\mathsf{J}^{-1} = \begin{bmatrix} -\mathrm{s}\phi/b & \mathrm{c}\phi/b & h[\mathrm{c}\beta\mathrm{c}\phi + \mathrm{s}\beta\mathrm{s}\phi]/b - 1 \\ \mathrm{c}\phi/r & \mathrm{s}\phi/r & h[\mathrm{c}\beta\mathrm{s}\phi - \mathrm{s}\beta\mathrm{c}\phi]/r \\ -\mathrm{s}\phi/b & \mathrm{c}\phi/b & h[\mathrm{c}\beta\mathrm{c}\phi + \mathrm{s}\beta\mathrm{s}\phi]/b \end{bmatrix}.$$

For compactness, we use s· and c· as shorthand for sin(·) and cos(·). It is interesting to note that the first two rows of J^{-1} express the nonholonomic constraints due to ideal rolling while the third row is a holonomic constraint: $\theta = \sigma - \phi$.

Using the joint space dynamics from eq. (1) and the inverse Jacobian in eq. (2), we can express the operational space dynamics of the ith manipulator as

$$\Lambda_i(\mathbf{w}_i)\ddot{\mathbf{x}} + \boldsymbol{\mu}_i(\mathbf{w}_i, \dot{\mathbf{w}}_i, \dot{\mathbf{x}}) = \mathbf{F}_i, \tag{3}$$

with

$$\Lambda_i = \mathsf{J}_i^{-T} A_i \mathsf{J}_i^{-1}$$

$$\boldsymbol{\mu}_i = \mathsf{J}_i^{-T}\left(A_i \dot{\mathsf{J}}_i^{-1}\dot{\mathbf{x}} + \mathbf{b}_i\right),$$

where Λ is the operational space mass matrix, $\boldsymbol{\mu}$ is the operational space vector of centripetal and Coriolis terms, and $\mathbf{F}$ is the force/torque vector at the origin of the end effector coordinate system. Since our manipulator is simple and not redundant, we compute J^{-1} directly, thus avoiding an inversion operation, which is traditionally required. Also note that as expressed here, $\boldsymbol{\mu}_i$ is a function of $\mathbf{w}_i$, $\dot{\mathbf{w}}_i$ and $\dot{\mathbf{x}}$. This representation allows us to use exact local information, such as the rolling speed of the wheel, which is measured directly, and to use the best estimates of the base speeds, which we develop in Section 4.

If we choose the end effector frames of the various manipulators such that they are coincident while the wheel modules are correctly positioned with respect to one another (see Fig. 5), then, using the augmented object model of Khatib (1988), we can write the overall operational space dynamics of the mobile base.

$$\Lambda\ \ddot{\mathbf{x}} + \boldsymbol{\mu} = \mathbf{F} \tag{4}$$

with

$$\Lambda = \sum_i^n \Lambda_i \quad ; \quad \boldsymbol{\mu} = \sum_i^n \boldsymbol{\mu_i} \quad ; \quad \mathbf{F} = \sum_i^n \mathbf{F}_i.$$

Here, Λ, $\boldsymbol{\mu}$, and $\mathbf{F}$ have the same meanings as before but now represent the properties of the entire robot.

With this algorithm, we have determined the operational space dynamic equations of motion directly. For our four-wheeled XR4000 robot, we generate 12 equations, 3 for each i in eq. (3), which are then added in groups of four to give the required 3 operational space equations. Using the symbolic dynamic equation generator AUTOLEV to create Λ and $\boldsymbol{\mu}$, the number of multiplications and additions are reduced from 8180 and 2244 to 2174 and 567.

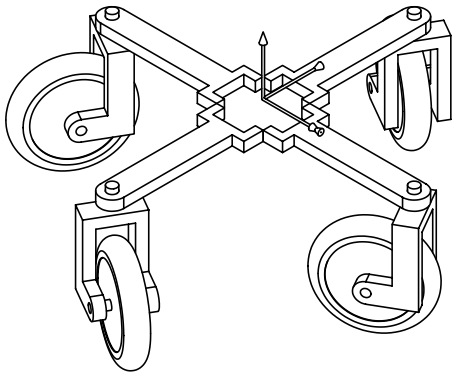

Fig. 5. Cooperating powered caster manipulators.

4. Dynamically Decoupled Control

The control and dynamic decoupling of the PCV is achieved by selecting the operational space control structure (Khatib 1987),

$$\mathbf{F} = \Lambda\ \mathbf{F}^* + \boldsymbol{\mu}, \tag{5}$$

where $\mathbf{F}$ is the operational space force that is to be applied to the PCV and $\mathbf{F}^*$ is the control force for our linearized unit mass system. As an example, we can choose to implement a simple proportional derivative controller

$$\mathbf{F}^* = -K_p(\mathbf{x} - \mathbf{x}_d) - K_v(\dot{\mathbf{x}} - \dot{\mathbf{x}}_d) + \ddot{\mathbf{x}}_d, \tag{6}$$

with K_p, K_v the position and velocity gains, and $\mathbf{x}_d$ and its derivatives the desired position, velocity, and acceleration.

This approach requires that we know the operational space velocities, $\dot{\mathbf{x}}$, of the PCV and the actuated robot joint torques, $\boldsymbol{\Gamma}$, necessary to produce the commanded operational space force, $\mathbf{F}$. The XR4000-powered casters (see Fig. 2) have an encoder on each motor. The encoders together with knowledge of the gearbox kinematics allow us to calculate the positions and velocities of the steering and rolling joints of each module. We can write the relationships between the observed robot joint speeds and the operational speeds of the ith wheel as the *wheel constraint matrix*, C_i, which contains the two nonholonomic constraints from "manipulator" model in eq. (2). We will use $\dot{\mathbf{q}}_i = [\,\dot{\phi}_i\ \ \dot{\rho}_i\,]^T$ to designate the observed joint speeds of the ith wheel.

$$\dot{\mathbf{q}}_i = C_i\ \dot{\mathbf{x}} \tag{7}$$

$$C_i = \begin{bmatrix} -\mathrm{s}\phi_i/b & \mathrm{c}\phi_i/b & h_i[\mathrm{c}\beta_i\mathrm{c}\phi_i + \mathrm{s}\beta_i\mathrm{s}\phi_i]/b - 1 \\ \mathrm{c}\phi_i/r & \mathrm{s}\phi/r & h_i[\mathrm{c}\beta_i\mathrm{s}\phi_i - \mathrm{s}\beta_i\mathrm{c}\phi_i]/r \end{bmatrix}.$$

The overall motion of the joints in the robot can be described by gathering the wheel constraint matrices into the *constraint matrix*, C.

$$\dot{\mathbf{q}} = C\ \dot{\mathbf{x}} \tag{8}$$

$$\dot{\mathbf{q}} = \begin{bmatrix} \dot{\mathbf{q}}_1 \\ \vdots \\ \dot{\mathbf{q}}_n \end{bmatrix} \quad ; \quad C = \begin{bmatrix} C_1 \\ \vdots \\ C_n \end{bmatrix}.$$

The dual of this relationship describes the operational space force produced by the torques at the actuated joints.

$$\mathbf{F} = C^T \, \mathbf{\Gamma}. \tag{9}$$

To find the operational space velocities and actuated joint torques, we need to find the inverse relationships to eqs. (8) and (9). One common approach is to use a generalized inverse (Muir and Neuman 1986) of the full constraint matrix C. Our approach instead involves two steps: finding the velocities at the contact points from the joint speeds and then resolving the contact point velocities to find the overall vehicle speeds. This provides a more physically intuitive solution to the inverse problem.

It may be easiest to visualize the contact point velocities as the speeds, $\dot{\mathbf{p}}$, that the contact points would have in the world if the robot body were held fixed and the wheels were not in contact with the ground. This is illustrated in Figure 6.

The sensed contact points velocities can be calculated from the measured joint speeds with the one-to-one mapping below where C_q is square, full rank, block diagonal, and invertible.

$$\dot{\mathbf{q}} = C_q \, \dot{\mathbf{p}}. \tag{10}$$

When the robot obeys the ideal rolling assumptions, there exists a vehicle velocity where the sensed contact speeds are identical to the consistent set of contact speeds, $\hat{\dot{\mathbf{p}}}$, found with the kinematic relationship

$$\hat{\dot{\mathbf{p}}} = C_p \, \dot{\mathbf{x}}. \tag{11}$$

However, as is to be expected, when there is some slippage and measurement noise, $\dot{\mathbf{p}} \neq \hat{\dot{\mathbf{p}}}$. By using the Moore-Penrose pseudo-inverse of the nonsquare matrix C_p, we get $\dot{\mathbf{x}} = C_p^+ \dot{\mathbf{p}}$, which will minimize the total perceived slip by minimizing the differences between $\dot{\mathbf{p}}$ and $\hat{\dot{\mathbf{p}}}$. Our estimate of the robot velocity assuming that slip is minimized uses a generalized inverse of the constraint matrix and is

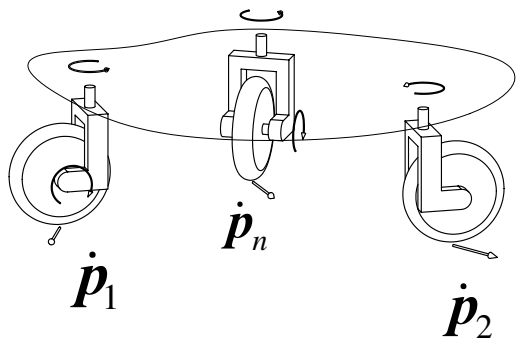

Fig. 6. Contact point velocities.

$$\dot{\mathbf{x}} = C_{qp}^{\#} \, \dot{\mathbf{q}}, \tag{12}$$

where

$$C_{qp}^{\#} = C_p^+ C_q^{-1}. \tag{13}$$

We have tested the odometry of our XR4000 moving randomly for 1 minute in a 1.5×2.5 m area and then returning to its starting position. When using the generalized inverse from eq. (13), the dead-reckoning error was less than half as large as when the pseudo-inverse of the constraint matrix was used.

The dual of this result is just as ideal. There are many ways to distribute the effort among the joints to achieve a desired operational space force. By distributing the joint torques using the transpose of the generalized inverse in eq. (13),

$$\mathbf{\Gamma} = C_{qp}^{\#^T} \, \mathbf{F}, \tag{14}$$

we minimize, in a least squares way, the contact forces developed by the wheels. The consequence is that the tractive effort is spread as evenly as possible among the wheels and the tendency for any one wheel to loose traction is minimized.

Other useful, physically meaningful generalized inverses can be found using the same methodology as follows. A one-to-one mapping from the velocities of interest to the measured velocities is derived. A second mapping, which goes from the operational speeds to the velocities of interest is derived. The product of the two mappings must equal the constraint matrix, C. The new generalized inverse of the constraint matrix is then the pseudo-inverse of the second matrix times the direct inverse of the first matrix.

A second useful example can be developed by mapping the measured and operational velocities to the motor speeds. The generalized inverse created with this mapping, when used to distribute the operational forces among the motors, minimizes the total power used by the motors. There have been problems in the past with using generalized inverses of Jacobians for manipulators because the meaning of minimizing quantities that have a combination of linear and angular units is not well defined. The two proposed generalized inverses do not suffer from this problem because the velocity vectors of interest have consistent units. Only linear units are present in the vector of contact velocities from the first example, while the speeds of interest in the second example have only angular units.

5. Experiments

5.1. Setup

Two experiments are presented. All experiments use a Nomadic Technologies XR4000, which is a four-wheeled, powered caster vehicle. The mobile manipulation experiment uses

a PUMA 560, which is mounted on the XR4000 as shown in Figure 1. The controller software was run on an on-board 450 MHz Pentium II, using the QNX real-time operating system. The mobile manipulation experiment was carried out with the addition of a fast dynamics algorithm developed and implemented by K. S. Chang in our lab (Chang 2000). All experiments were run using the controller structure shown in Figure 7 for the PCV control, with a 1000 Hz servo rate for all calculations. All experiments were run fully autonomously with the robot using its on-board batteries for power and radio Ethernet for communication.

5.2. PCV Dynamic Decoupling

The first experiment demonstrates the effectiveness of the proposed dynamically decoupled, dynamic control of a PCV. In this experiment, the robot was commanded to move from its starting location, $(x, y, \theta) = (0, 0, 0)$, to 1 meter in the y direction, $(x, y, \theta) = (0, 1, 0)$, and then back again, repeatedly. The robot was commanded to follow a straight line path without rotation, that is, $x = 0$ and $\theta = 0$. The maximum acceleration magnitude was limited to 1.0 m/s^2. The gains used in this experiment were reduced by a factor of 10 from the typical gains used during normal motions so that dynamic disturbances would be more apparent.

The desired position and velocity for the only changing coordinate, y, are shown with the dashed lines in Figure 8. Each time the XR4000 changes direction in this task, all four wheels must flip their orientations (see Fig. 9), and in doing so, cause large dynamic coupling forces. The good performance, in spite of reduced gains, recorded by the solid lines in Figure 8, are a result of compensating for the coupled dynamics of the mechanism. To illustrate the importance of the role decoupling plays, Figure 10 shows the compensation used for the x and θ joints of the PCV. Notice that the magnitude of the dynamic x disturbance force reaches 600 N and the dynamic θ disturbance torque reaches 100 N·m—significant disturbances, even for a 160 kg robot.

In Figures 11 and 12, some of the disturbance effects of the dynamic forces are shown. In Figure 11, the robot was run without using dynamic compensation and has position errors in the order of 30 mm and 3 deg. In Figure 12, the robot was run while implementing the proposed dynamic compensation and the errors are reduced to about 5 mm and 0.5 deg.

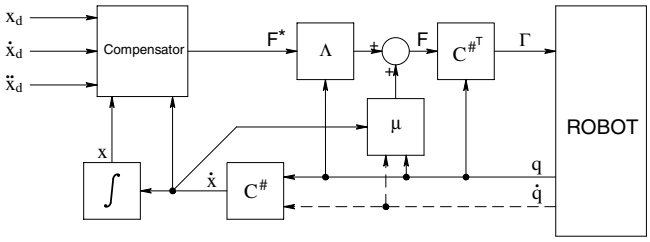

Fig. 7. Controller schematic.

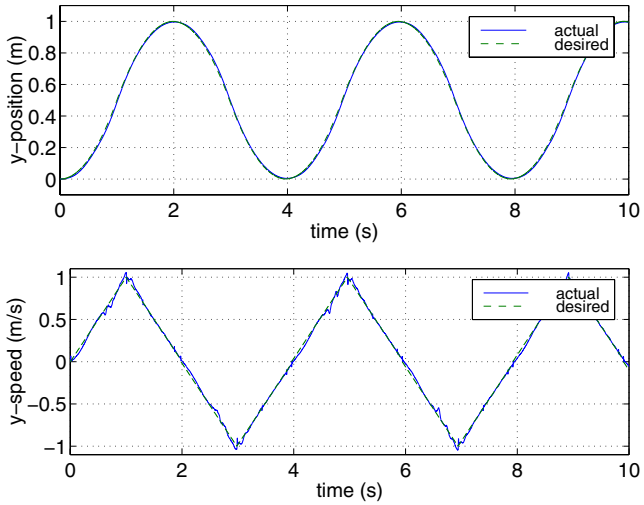

Fig. 8. Position versus time and velocity versus time with dynamic compensation.

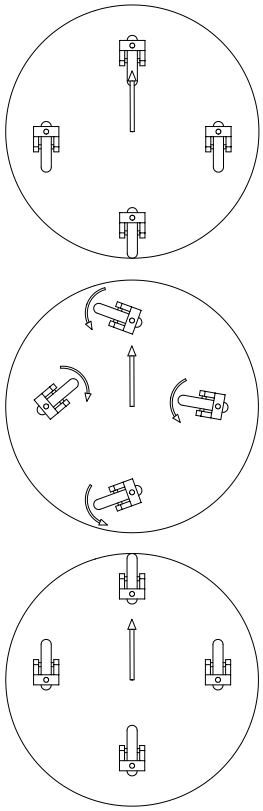

Fig. 9. Wheel "flip" during y-axis motion, which leads to large dynamic disturbance forces.

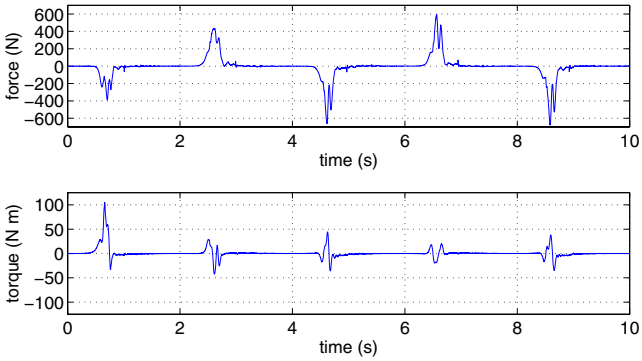

Fig. 10. Dynamic compensation force-x and dynamic compensation torque-θ.

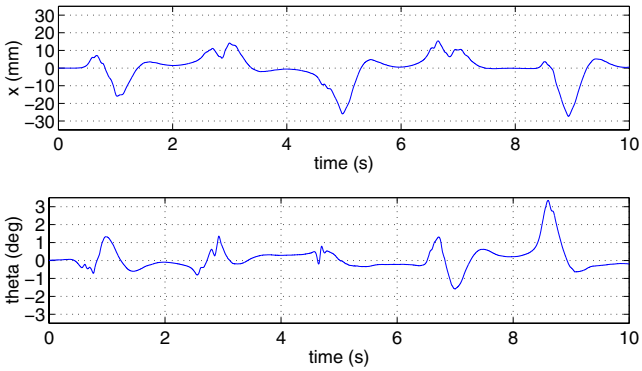

Fig. 11. Positions without dynamic compensation.

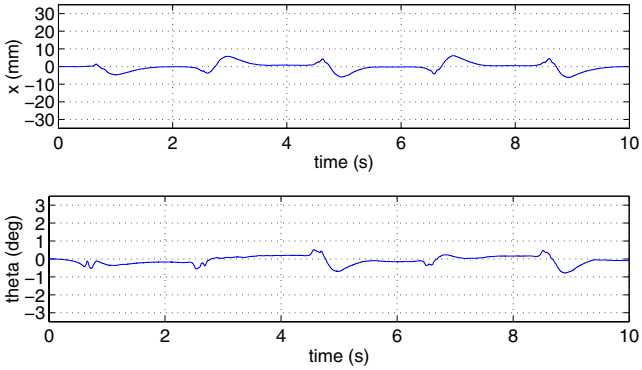

Fig. 12. Positions with dynamic compensation.

5.3. Mobile Manipulator Coordination

The second experiment shows the effectiveness of using operational space control on the mobile robot when it is acting as the base joints of the mobile manipulator robot system. In this experiment, the PCV, which we will call the *base* in this context, was commanded to travel from the original location, $(x, y, \theta) = (0, 0, 0)$, to 2 meters in the y direction, $(x, y, \theta) = (0, 2, 0)$. The PUMA 560 was set to begin in the "home" position with joint 2 level and pointing in the y direction and joint 3 vertical and pointing upward. When the motion was started, the PUMA was commanded to wave its arm by moving joint 1 (waist) between 0.0 and 0.6 radians (34.4 deg) at 0.95 Hz (6.0 rad/sec) in a sinusoidal trajectory. This trajectory is shown in Figures 13 and 14. Dynamic decoupling is used for the motions shown in these two figures.

The rapid waving of the PUMA arm caused large dynamic disturbance torques particularly to the orientation of the base. Again, the gains used in this experiment were reduced by a factor of 10 from the typical gains used during normal motions so that dynamic disturbances would be more apparent. The orientation errors of the base are shown in Figure 15. Without dynamic compensation, the orientation of the base has errors of about ± 6 deg, while with dynamic compensation for the disturbance forces generated by the PUMA, the orientation error is reduced to less than ± 1 deg.

6. Conclusions

We have presented the design of a new wheeled holonomic mobile robot, the PCV, which is being produced as the XR4000 mobile robot by Nomadic Technologies. The design of the PCV provides smooth accurate motion with the ability to traverse the hazards of typical indoor environments. The design can be used with two or more wheels, and as

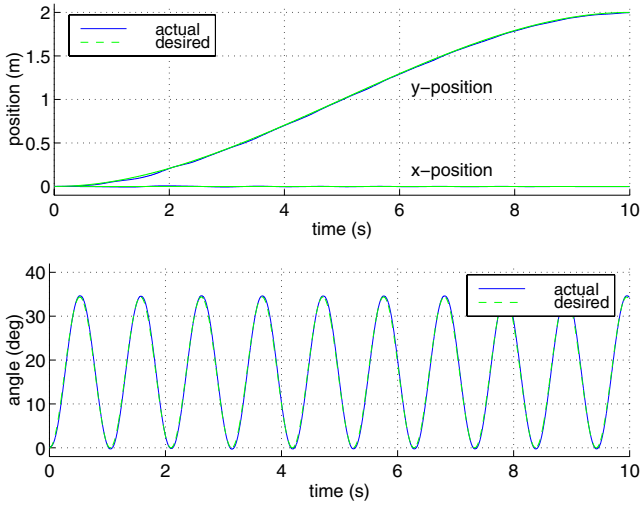

Fig. 13. Base x and y positions versus time and PUMA joint 1 angle versus time.

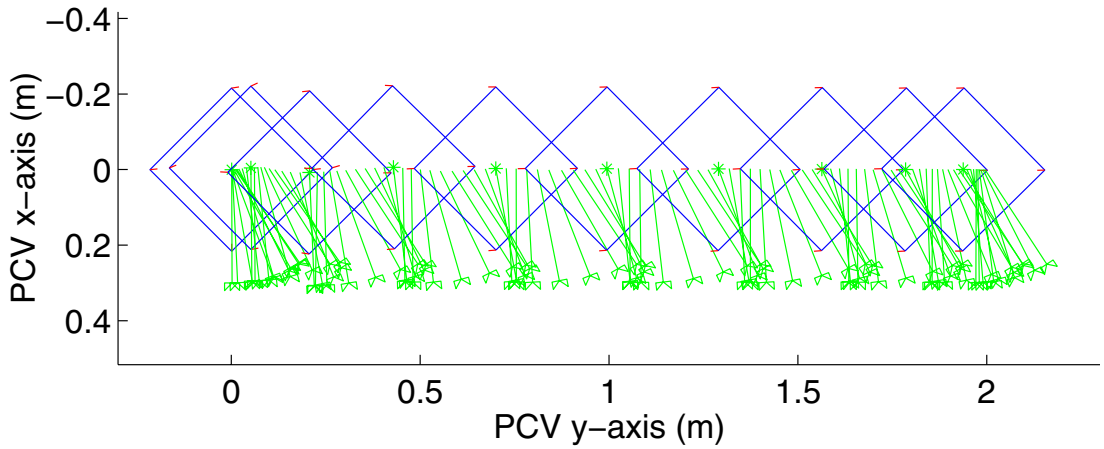

Fig. 14. Path of robot and manipulator arm.

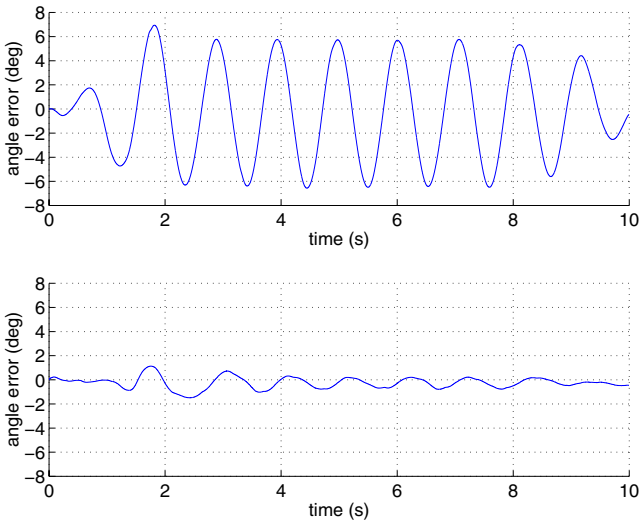

Fig. 15. Base orientation error without and with dynamic compensation.

implemented with four wheels provides a stable platform for mobile manipulation.

We have also described a new approach for a modular, efficient dynamic modeling of wheeled vehicles. This approach is based on the augmented object model originally developed for the study of cooperative manipulators. The actuation redundancy is resolved to effectively distribute the actuator torques to minimize internal or antagonistic forces between wheels. This results in reduced wheel slip and improved odometry.

Using the vehicle dynamic model and the actuation and measurement redundancy resolution, we have developed a control structure that allows vehicle dynamic decoupling and slip minimization. The effectiveness of this approach was experimentally demonstrated for motions involving large dynamic effects.

The PCV dynamic model and control structure have been integrated into a new mobile manipulation platform integrating the XR4000 and a PUMA arm. The experimental results on the new platform have shown full dynamic decoupling and improved performance.

Acknowledgments

We gratefully acknowledge Nomadic Technologies, Inc., where the development of the powered caster mechanism took place; for the primary financial support of this project, and to the work of all the individuals there, especially Anthony del Balso, Rich Legrand, Jim Slater, and John Slater who were instrumental in the creation of the XR4000 mobile robot. The financial support of Boeing and Honda is gratefully acknowledged. Thanks also to K. C. Chang for development of the mobile manipulation controller software in which the PCV controller was integrated.

References

Bradbury, H. M. 1977 (December). Omni-directional transport device. U.S. Patent #4223753.

Campion, G., Bastin, G., and d'Andréa-Novel, B. 1993. Structural properties and classification of kinematic and dynamic models of wheeled mobile robots. *Proc. IEEE International conference on Robotics and Automation*, Atlanta, GA, May, pp. 462–469.

Carlisle, B. 1983. An omni-directional mobile robot. In *Developments in Robotics*, ed. B. Rooks, 79–87. Kempston, UK: IFS.

Chang, K.-S. 2000 (March). *Efficient Algorithms for Articulated Branching Mechanisms: Dynamic Modeling, Control, and Simulation*. Ph.D. thesis, Stanford University, Stanford, CA.

Craig, J. J. 1989. *Introduction to Robotics*. 2d ed. Menlo Park, CA: Addison-Wesley.

Hirose, S., and Amano, S. 1993. The VUTON: High payload high efficiency holonomic omni-directional vehicle. *6th International Symposium on Robotics Research*, Pittsburgh, PA, October, pp. 253–260.

Ilon, B. E. 1971 (December). Directionally Stable Self Propelled Vehicle. U.S. Patent #3746112.

Khatib, O. 1987 (February). A unified approach for motion and force control of robotic manipulators: The operational space formulation. *IEEE Journal of Robotics and Automation* RA-3(1):43–53.

Khatib, O. 1988. Object manipulation in a multi-effector robot system. In *Robotics Research 4 Proc. 4th Int. Symposium*, 137–144. Cambridge, MA: MIT Press.

Khatib, O., Brock, O., Yokoi, K., and Holmberg, R. 1999. Dancing with Juliet 1999. *IEEE Robotics and Automation Conference Video Proceedings*, Detroit, MI.

Khatib, O., and Yokoi, K., Brock, O., Chang, K., and Casal, A. 1999. Robots in human environments: Basic autonomous capabilities. *International Journal of Robotics Research* 18:684–696.

Khatib, O., Yokoi, K., Chang, K., Ruspini, D., Holmberg, R., and Casal, A. 1996. Proceedings of the IEEE/RSJ International Conference on Intelligent Robots and Systems. In *Vehicle/Arm Coordination and Multiple Mobile Manipulator Decentralized Cooperation*, Osaka, Japan, vol. 2, pp. 546–553.

Killough, S. M., and Pin, F. 1992. Design of an omnidirectional and holonomic wheeled platform prototype. *Proc. IEEE International Conference on Robotics and Automation*, Nice, France, May, vol. 1, pp. 97–103.

La, H. T. 1979 (January). Omnidirectional Vehicle. U.S. Patent #4237990.

Muir, P. F., and Neuman, C. P. 1986 (June). Kinematic modeling of wheeled mobile robots. Technical Report CMU-RI-TR-86-12, The Robotics Institute, Carnegie-Mellon University, Pittsburgh, PA.

Pin, F. G., and Killough, S. M. 1994 (August). A new family of omnidirectional and holonomic wheeled platforms for mobile robots. *IEEE Transactions on Robotics and Automation* 10(4):480–489.

Wada, M., and Mori, S. 1996. Holonomic and omnidirectional vehicle with conventional tires. *Proc. IEEE International Conference on Robotics and Automation*, Minneapolis, MN, April, pp. 3671–3676.

West, M., and Asada, H. 1992. Design of a holonomic omnidirectional vehicle. *Proc. IEEE International Conference on Robotics and Automation*, Nice, France, May, pp. 97–103.

West, M., and Asada, H. 1994. Design of ball wheel vehicles with full mobility, invariant kinematics and dynamics and anti-slip control. *Proceedings of the ASME Design Technical Conferences, 23rd Biennial Mechanisms Conference ASME*, Minneapolis, MN, vol. 72, pp. 377–384.